Journal of Cerebral Blood Flow & Metabolism (2012) 32, 1177–1187

www.jcbfm.com

Review Article

Brain energy metabolism and blood flow differences in healthy aging

Joel Aanerud[1], Per Borghammer[1], M Mallar Chakravarty[2,3], Kim Vang[1], Anders B Rodell[1], Kristjana Y Jónsdottir[4], Arne Møller[1,4], Mahmoud Ashkanian[1,4], Manouchehr S Vafaee[1,5], Peter Iversen[1], Peter Johannsen[6] and Albert Gjedde[1,4,5,7,8,9]

[1]*Department of Nuclear Medicine and PET Centre, Aarhus University Hospital, Aarhus, Denmark;* [2]*Rotman Research Institute, Baycrest Hospital, Toronto, Ontario, Canada;* [3]*Mouse Imaging Centre, The Hospital for Sick Children, Toronto, Ontario, Canada;* [4]*Center of Functionally Integrative Neuroscience, University of Aarhus, Aarhus, Denmark;* [5]*Department of Neuroscience and Pharmacology, University of Copenhagen, Copenhagen, Denmark;* [6]*Memory Disorders Research Unit, Department of Neurology, Copenhagen University Hospital, Copenhagen, Denmark;* [7]*Center for Healthy Aging, University of Copenhagen, Copenhagen, Denmark;* [8]*McConnell Brain Imaging Center, Montreal Neurological Institute, McGill University, Montreal, Quebec, Canada;* [9]*Department of Radiology and Radiological Science, Johns Hopkins University, Baltimore, Maryland, USA*

Cerebral metabolic rate of oxygen consumption (*CMRO$_2$*), cerebral blood flow (*CBF*), and oxygen extraction fraction (*OEF*) are important indices of healthy aging of the brain. Although a frequent topic of study, changes of *CBF* and *CMRO$_2$* during normal aging are still controversial, as some authors find decreases of both *CBF* and *CMRO$_2$* but increased *OEF*, while others find no change, and yet other find divergent changes. In this reanalysis of previously published results from positron emission tomography of healthy volunteers, we determined *CMRO$_2$* and *CBF* in 66 healthy volunteers aged 21 to 81 years. The magnitudes of *CMRO$_2$* and *CBF* declined in large parts of the cerebral cortex, including association areas, but the primary motor and sensory areas were relatively spared. We found significant increases of *OEF* in frontal and parietal cortices, excluding primary motor and somatosensory regions, and in the temporal cortex. Because of the inverse relation between *OEF* and capillary oxygen tension, increased *OEF* can compromise oxygen delivery to neurons, with possible perturbation of energy turnover. The results establish a possible mechanism of progression from healthy to unhealthy brain aging, as the regions most affected by age are the areas that are most vulnerable to neurodegeneration.
Journal of Cerebral Blood Flow & Metabolism (2012) **32,** 1177–1187; doi:10.1038/jcbfm.2012.18; published online 29 February 2012

Keywords: aging; energy metabolism; neurovascular coupling; positron emission tomography

Introduction

Oxygen metabolism in brain (*CMRO$_2$*), cerebral blood flow (*CBF*), and oxygen extraction fraction (*OEF*) in the brain are important indices of healthy aging. Here we review, by means of novel reanalysis, the results of several recent studies of these variables in healthy volunteers, performed by the authors and reported in the literature. This reanalysis follows the practice of (Kety, 1956) who reviewed the first 10 years of results obtained with the nitrous oxide technique of Kety and Schmidt (1945, 1948). The author reported significant declines of whole-brain values of *CBF* and *CMRO$_2$*, as well as an increase of *OEF* with increasing age. Positron emission tomography (PET) later made it possible to study subdivisions of the brain, and several studies revealed regional decreases of both *CBF* (Borghammer *et al*, 2008; Leenders *et al*, 1990; Lenzi *et al*, 1981; Marchal *et al*, 1992; Martin *et al*, 1991; Pantano *et al*, 1984) and *CMRO$_2$* (Ibaraki *et al*, 2010; Leenders *et al*, 1990;

Correspondence: Professor A Gjedde, Department of Neuroscience and Pharmacology, Panum Institute, Faculty of Medicine and Health Sciences, University of Copenhagen, 2200 Copenhagen, Denmark.
E-mail: gjedde@sund.ku.dk
This study was supported by the center-of-excellence Grants from Aarhus University and the Danish National Research Foundation (Danmarks Grundforskningsfond), as well as by the granting agencies acknowledged in the publications reviewed here.
Received 7 October 2011; revised 21 December 2011; accepted 21 December 2011; published online 29 February 2012

Lenzi *et al*, 1981; Marchal *et al*, 1992; Takada *et al*, 1992; Yamaguchi *et al*, 1986). However, a few authors reported no changes or equivocal results for *CBF* (Ibaraki *et al*, 2010; Meltzer *et al*, 2000; Takada *et al*, 1992; Yamaguchi *et al*, 1986) and $CMRO_2$ (Burns and Tyrrell, 1992; Pantano *et al*, 1984). Of the cited studies, four included calculations of *OEF*, but only Leenders *et al* (1990) reported significant increase with age, while the remainder of the studies (Ibaraki *et al*, 2010; Marchal *et al*, 1992; Pantano *et al*, 1984) failed to replicate Kety's early observation.

To some observers, the apparent lack of change of *OEF* in conditions of steady state of the healthily aging brain indicates a close match of *CBF* to the metabolic demands of neurons, while to other observers, the optimal oxygen homeostasis requires a nonlinear relation between $CMRO_2$ and *CBF* (Gjedde *et al*, 2005). Relative changes of $CMRO_2$ and *CBF*, reflected in the *OEF*, determine the pressure gradients of oxygen delivery. During activations of the brain, decreases of the *OEF* generally benefit the oxygen homeostasis in brain tissue because they elevate the average partial pressure of oxygen in capillaries (Buxton and Frank, 1997). Conversely, the same mechanism, operating under conditions of possible deactivation of brain tissue as a consequence of aging, hence may lead to a rise of *OEF*, although evidence is lacking for this contingency. Thus, if $CMRO_2$ remains constant during healthy aging, a reduction of *CBF* that exceeds the normal decline in response to reduced metabolic demand necessarily leads to an abnormally large increase in *OEF*. Also, an increase of *OEF* at rest with no change of $CMRO_2$ would signify a perturbed regulation of blood flow, at variance with the underlying hypothesis that *CBF* is adjusted to maintain oxygen tensions consistent with the oxygen demands of the neurons. Therefore, we predict that elevated *OEF* can impose a limitation on the delivery of oxygen, when average oxygen tensions decline in capillaries as well as in the tissue (Gjedde *et al*, 2005, 2010).

Early PET studies obtained the values of parametric variables from tomographic records with 16 mm isotropic resolution. Spatial resolution of this magnitude limits accurate estimation of *CBF* and $CMRO_2$ because of signal dispersion to white matter and cerebrospinal fluid, as the cerebral cortex is only 2.5 to 3 mm thick (Pakkenberg and Gundersen, 1997; Rabinowicz *et al*, 2002). This signal dispersion generates the well-known partial volume effect (PVE) of signal dilution. The widening of sulcal spaces during normal aging further compounds the PVE-based bias. However, the improved spatial resolution of modern tomographs allows more accurate estimates of *CBF* and $CMRO_2$ than previously possible and thus attenuates the bias introduced by aging. Importantly, *OEF* will not be affected by PVE, since it is calculated as a ratio between $CMRO_2$ and *CBF*, rather than being measured directly.

Another improvement is statistical parametric mapping, which yields voxel-wise rather than region-wide parametric estimates. This method has the potential of objectively identifying areas of significant change, independently of the volumes-of-interest (VOIs) chosen by the investigators.

Inspired by these limitations and the contradictory or uncertain results of previous studies, we chose to reexamine the adequacy of flow–metabolism coupling for oxygen delivery during healthy aging within a sufficiently large population of healthy volunteers studied with higher-resolution PET instrumentation and up-to-date data analysis. By application of these improved methods, compared with older studies, we expected to find changes of *CBF*, $CMRO_2$, and *OEF* with higher significance than previously obtained.

Subjects and methods

Subjects

Sixty-six healthy subjects (46 males) aged 21 to 81 years volunteered for the studies included in this reanalysis. Originally excluded were subjects with neurologic or psychiatric disorders by clinical interview and examination. The volunteers took no medication or substances with known effects on brain–blood flow or metabolism. Complete details on the subjects, who had participated in earlier studies, were published previously (Ashkanian *et al*, 2009; Borghammer *et al*, 2008; Gjedde *et al*, 2005; Iversen *et al*, 2009; Møller *et al*, 2006). Written informed consent was obtained from all subjects and the protocols were approved by the regional Science Ethics Committee, in accordance with the declaration of Helsinki.

Magnetic Resonance Imaging

Thirty-eight of the subjects had T1-weighted scans obtained on a 3.0 T Signa Excite GE Magnet using a 3DIR-fSPGR sequence (256×256, echo time (TE)1 = min full, time of inversion (TI) = 450, slice thickness = 1.5 mm) and 28 subjects were scanned with GE MR 1.5-T Echo Speed tomograph (3D-SPGR, 256×256, 1 Splap, number of excitations (NEX): 1, slice thickness 1.5).

Positron Emission Tomography Examinations

Sixty-five subjects had one dynamic $[^{15}O]H_2O$ emission recording, and 65 had one or two $[^{15}O]O_2$ emission recordings. All recordings were performed with the subjects resting in a supine position in a quiet room with eyes open, except in one study where subjects had their eyes closed. Recordings were acquired in 3D mode with the ECAT EXACT HR47 (CTI/Siemens, Knoxville, TN, USA) whole-body tomograph. The image volumes had an isotropic resolution of 4.6 mm. Images were reconstructed as 128×128 matrices of $2 \times 2\,mm^2$ voxels using filtered back projections with a 0.5 per cycle Hann filter. The reconstructed images were corrected for random and scatter events, detector efficiency variations, and dead time. Tissue attenuation scans were performed using a rotating ^{68}Ge source. Dynamic emission

recordings lasting 3 minutes (21 frames) were initiated on bolus intravenous injection of $[^{15}O]H_2O$ (500 MBq) or inhalation of $[^{15}O]O_2$ (500 or 1,000 MBq). Catheters (Artflon and Venflon, Becton Dickinson, Swindon, UK) were inserted in the left radial artery and right cubital vein. In all, 50 subjects had arterial blood radioactivity measured by an automated blood sampling system (Allogg AB, Mariefred, Sweden), crosscalibrated with the tomograph, and then corrected for external delay and dispersion. Remaining subjects had arterial blood samples manually drawn to measure radioactivity (21 samples: 12×5, 6×10, and 3×20 seconds).

Image Processing

The dynamic PET recordings were smoothed to a full-width half-maximum (FWHM) of 6 mm. As labeled water is assumed to undergo rapid distribution in the entire brain tissue volume, the model used to analyze the images had only one tissue compartment. Parametric images of the unidirectional blood–brain clearance of either tracer were calculated with the single-step modified linearizations of the one tissue compartment model of (Blomqvist, 1984) described by Ohta *et al* (1992, 1996) with Lawson and Hanson (1974) nonnegative least squares solutions of general least squares functions. For *CBF*, the model yields estimates of K_1 and k_2 constants for the diffusion of $[^{15}O]H_2O$ between the blood and brain tissue compartments. With correct inclusion of a blood compartment Raichle *et al* (1983) show that for blood flow < 55 mL/100 g per minute (close to the current average), the estimated water clearance from the blood can be regarded as 100% of the true clearance, such that K_1 consequently equals *CBF*. For $CMRO_2$, the model estimates the magnitudes of the clearance K_1 and the rate constant k_2 for the diffusion of $[^{15}O]O_2$ between the two compartments. It is assumed that oxygen 'instantly' is metabolized to water, which is freely diffusible between the two compartments. However, the implementation of Ohta *et al* (1996) does not make use of the k_2 estimate.

We did spatial coregistration in two separate ways. The first method derived VOIs; individual MR images were warped to fit (Collins *et al*, 1995; Collins and Evans, 1997) a template based on 85 brains from young healthy people in ICBM152 space (http://imaging.mrc-cbu.cam.ac.uk/imaging/MniTalairach). A linear transformation was estimated and then used as input to a nonlinear transformation estimation process to accurately match anatomy between the subject and the template with a hierarchical transformation estimation strategy. Summed PET images were coregistered to individual MR images, and the concatenated transformation files were applied to the dynamic PET images. The second method of coregistration was chosen with the specific purpose of voxel-based statistics; Individual *CBF* PET images were registered directly to a *CBF*-PET atlas (*SPM2*, London, UK). Cerebral metabolic rate of oxygen consumption PET images were coregistered to each individual's *CBF* images. As above, all images were matched to the *CBF*-PET atlas with a linear transformation used as input to a hierarchical nonlinear transformation estimation strategy. Rigid body transformations matching the $CMRO_2$ to *CBF* images were concatenated with each of the *CBF*-to-atlas transformations.

Data Analysis

Volume-of-Interest Analysis: The automated coregistration algorithm extracted a binary mask of cortical gray matter (GM) from each individual's MR image. These binary masks were then multiplied with generic masks for each VOI, yielding individualized masks for all VOIs. The GM masks were manipulated (isotropic smoothing FWHM 4 mm, threshold 0.4) to be of approximately the same thickness as the PET signal from cortical GM (Figure 1). These were used to extract mean GM values from parametric PET images. Where subjects had two $CMRO_2$ images (average time between image acquisition 14 (s.d. 4.3) minutes), we used an average of the two (23 subjects). The cortical GM was divided into five VOI's: frontal lobe excluding the M1 area (F-M1), parietal lobe excluding the S1 area (P-S1), temporal lobe (T), primary motor and sensory cortex (M1S1), and occipital lobe (O)). Regression coefficients with age as an independent variable and *y*-intercepts at age 50 were calculated for *CBF*, $CMRO_2$, and *OEF*. First, a mixed model multilinear regression was performed on logarithmically transformed data to account for differences in mean *CBF* values among groups of subjects included from earlier studies. Individual PET images were then corrected for group differences, and a linear regression analysis with age as an independent variable, was performed in all VOIs. $PaCO_2$ has been found to positively correlate with *CBF* (Ito *et al*, 2000). Therefore, $PaCO_2$ was added as an independent variable in the regression analysis for *CBF*. Calculations were performed in STATA IC 10 for Mac (College Station, TX, USA).

Voxel-Based Analysis: Coregistered parametric images were normalized with the reference cluster method (Borghammer *et al*, 2009*a*; Yakushev *et al*, 2009). To use this method, we assumed that no brain region displays true

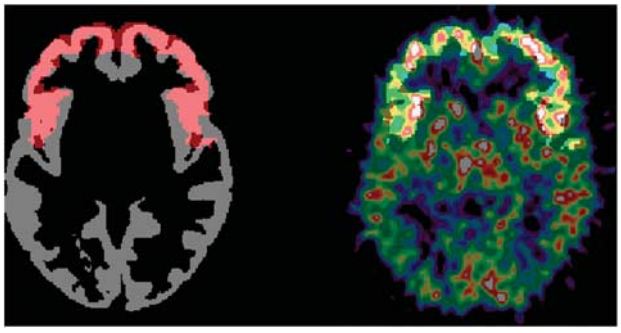

Figure 1 Illustration of the volume-of-interest (VOI) generation. On the left is shown a gray matter segmentation (gray) for a young subject with the generic mask for F-M1 (frontal lobe without primary motor area) (shown in red) overlaid. These binary masks are multiplied to create the VOI and are shown on the right (white). This customized VOI is superimposed on the parametric cerebral blood flow (*CBF*) image of the same subject.

increases as a result of aging in neither *CBF* nor $CMRO_2$. This assumption is justified since no previous quantitative PET study of aging reported absolute increases in perfusion or metabolism anywhere in the brain. Normalized images were blurred to a FWHM of $12 \times 12 \times 12\,mm^3$ and analyzed in *fMRIstat* (http://www.math.mcgill.ca/keith/fmristat) on MATLAB v 7.7.0 (R2008b) (The MathWorks, Natick, MA, USA). The method has been described elsewhere (Borghammer *et al*, 2009*b*). A linear regression model with age as an independent variable was fitted in each voxel for either *CBF* or $CMRO_2$. The program *fMRIstat* assigns a *t*-value in each voxel to reveal the significance of age with the dependent variables using the mixed effect model analysis described by Worsley *et al* (2002). After the model estimation, *t*-contrasts were specified to test statistical significance, and the resulting statistical maps were thresholded at $P < 0.05$, corrected for multiple comparisons using Gaussian Random Field Theory in the entire search area (Worsley *et al*, 1996).

Mean Cerebral Blood Flow and Cerebral Metabolic Rate of Oxygen Consumption in Age Groups

Parametric *CBF* (adjusted for study and $PaCO_2$) and $CMRO_2$ (adjusted for study) images were divided into three age groups aged 21 to 39 years ('young,' $n = 25$); 40 to 59 years ('middle age,' $n = 19$); and 60 to 81 years ('old,' $n = 21$) and mean images calculated in *fMRIstat*. Further analysis was performed on data divided into these age groups by extracting mean values in different VOIs from these images, separately for each hemisphere.

Calculation of Oxygen Extraction Fraction

Oxygen extraction fraction was calculated by the following formula:

$$OEF = \frac{CMRO_2}{CBF \bullet CaO_2}$$

where CaO_2 is the arterial content of oxygen (CaO_2 = hemoglobin concentration ● oxygen saturation) (Mintun *et al*, 1984).

Results

Three Age Groups

The average maps of the three age groups of $CMRO_2$ and *CBF* in the three age groups are shown in Figure 2. They show clear patterns of cortical decrease of *CBF* that are apparent both from young-to-middle age and from middle-to-advanced age. Subcortical structures appeared to maintain relatively constant values of *CBF* with aging. The images of $CMRO_2$ show some decline in cortex with aging, but the effect is relatively modest compared with the changes of *CBF*.

Volume-of-Interest Analysis

As listed in Table 1, values of *CBF* declined significantly in prefrontal and premotor regions of the frontal lobe in front of the motor cortex (F-M1) and in associative regions of the parietal lobe (P-S1),

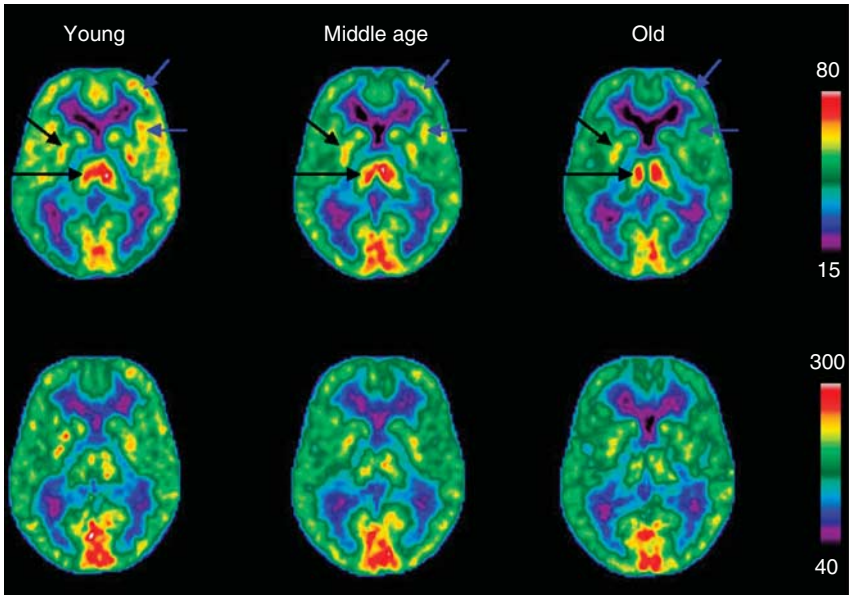

Figure 2 Top row shows mean cerebral blood flow (*CBF*) (mL/100 g per minute) images where cortical decreases are apparent both between young and middle age, and between middle age and old (blue arrows show examples). Subcortical structures are relatively conserved with aging (black arrows). Cerebral metabolic rate of oxygen (μmol/100 g per minute) images are shown in the bottom row, and although there is some cortical decline with aging, the effect is relatively small compared with the change in *CBF*. Left in the figure corresponds to left side of the brain.

Table 1 *CBF*, $CMRO_2$, and *OEF* values

Cortical region	CBF			$CMRO_2$			OEF		
	Mean at age 50	α	P *value of* α	*Mean at age 50*	α	P *value of* α	*Mean at age 50*	α	P *value of* α
F-M1	49	−0.18	<0.001	170	−0.31	0.031	0.41	0.001	0.014
P-S1	49	−0.14	0.006	179	−0.28	0.064	0.43	0.001	0.031
T	45	−0.12	0.007	166	−0.24	0.065	0.44	0.001	0.031
O	51	−0.05	0.336	200	−0.18	0.323	0.46	0.001	0.254
M1S1	46	−0.10	0.018	171	−0.19	0.192	0.43	0.001	0.063

CBF, cerebral blood flow; $CMRO_2$, cerebral metabolic rate of oxygen consumption; F-M1, frontal lobe without primary motor area; M1S1, primary motor and somatosensory area; O, occipital lobe; *OEF*, oxygen extraction fraction; P-S1, parietal lobe without primary somatosensory area; T, temporal lobe.
Mean parametric values at age 50, *CBF* (mL/100 g per minute), $CMRO_2$ (μmol/100 g per minute). α is the coefficient for the linear regression of *CBF*, $CMRO_2$, and *OEF* with age as independent variable.

as well as in temporal (T) and primary motor and sensory (M1S1) cortices. Values of $CMRO_2$, declined significantly only in F-M1, but tended toward significant declines in both P-S1 and temporal cortex. The magnitude of *OEF* increased significantly in F-M1, P-S1, and temporal cortex, and tended toward increase in M1S1. In Figure 3, we show scatter plots of the values of *CBF*, $CMRO_2$, and *OEF* for the regions F-M1, P-S1, temporal cortex, M1S1, and occipital lobe; the frontal lobe in front of motor cortex (F-M1) was the most severely affected region, while values in occipital lobe were unchanged. We note that the variation is considerable, also after correction for the effect of $PaCO_2$ on *CBF*. Analysis was also performed on data divided into three age groups (see above) for each VOI in each hemisphere and for each hemisphere globally. Results are shown in Table 2. The relationships between *CBF*, $CMRO_2$, and *OEF* in the three age groups generally show the same trend as the regression analysis.

Voxel-Based Analysis

The voxel-wise regression revealed changes that generally matched the regional results, with the statistically most significant decreases of *CBF* in anterior cingulate and the medial part of the superior frontal gyrus, and additional decreases in regions of lateral thalamus, pons, medulla oblongata, cerebellum, occipital lobes, and the superior parts of M1S1 (maximum *t*-value 11.02, $x=6$, $y=48$, $z=27$, cluster size 1297548 voxels). The decreases of $CMRO_2$ reached the highest levels of significance in the anterior part of the cortex, with less significant declines in subcortical regions of thalamus, caudate, and putamen, while values in white matter, cerebellum, brain stem, and occipital cortex, generally remained unchanged (maximum *t*-value 10.24, $x=10$, $y=46$, $z=24$, cluster size 1363296 voxels).

We present these results of the reanalysis in Figure 4 as Student's *t*-maps, where only significant changes in *CBF* and $CMRO_2$ are shown. In each voxel, regression coefficients of declining *CBF* or $CMRO_2$ values as a result of age were tested against the null hypothesis that the regression coefficient is zero. We give the results of these tests as Student's *t*-values, indicating the degree of significance.

Discussion

Estimates of Cerebral Blood Flow and Cerebral Metabolic Rate of Oxygen Consumption

In the review and reanalysis of studies of brain energy metabolism reported by this group for healthy volunteers studied at the Aarhus PET Center, we addressed the question of whether or not the variables of *CBF*, $CMRO_2$, and *OEF* change as functions of normal aging. To answer the question, we reanalyzed PET data from a large population of volunteers of different ages participating in different studies. To our knowledge, it thus became the first voxel-based analysis of changes of $CMRO_2$ during aging. We now report that values of *CBF* declined to a greater extent than values of $CMRO_2$, with consequent increase of the magnitudes of *OEF* in specific parts of the human brain. According to Nemoto *et al* (2003), values of *OEF* that exceed 0.60 are so high that they represent potentially pathological declines of oxygen delivery. The increases of the values of *OEF* in associative areas of the brain in the present data therefore imply that oxygen delivery may indeed approach that threshold with increasing age. The reason for the effect is the inverse relation between extraction and delivery of oxygen that was first described by Suwa (1992*a*, *b*) who explained how the increased oxygen extraction lowers the average tension of oxygen in capillaries and hence adversely affects the pressure gradient.

This explanation is now the canonical explanation of the beneficial effects of nonlinear coupling of blood flow and oxygen consumption changes during activations and deactivations of brain tissue (Gjedde, 1997; Buxton and Frank, 1997; Vafaee and Gjedde,

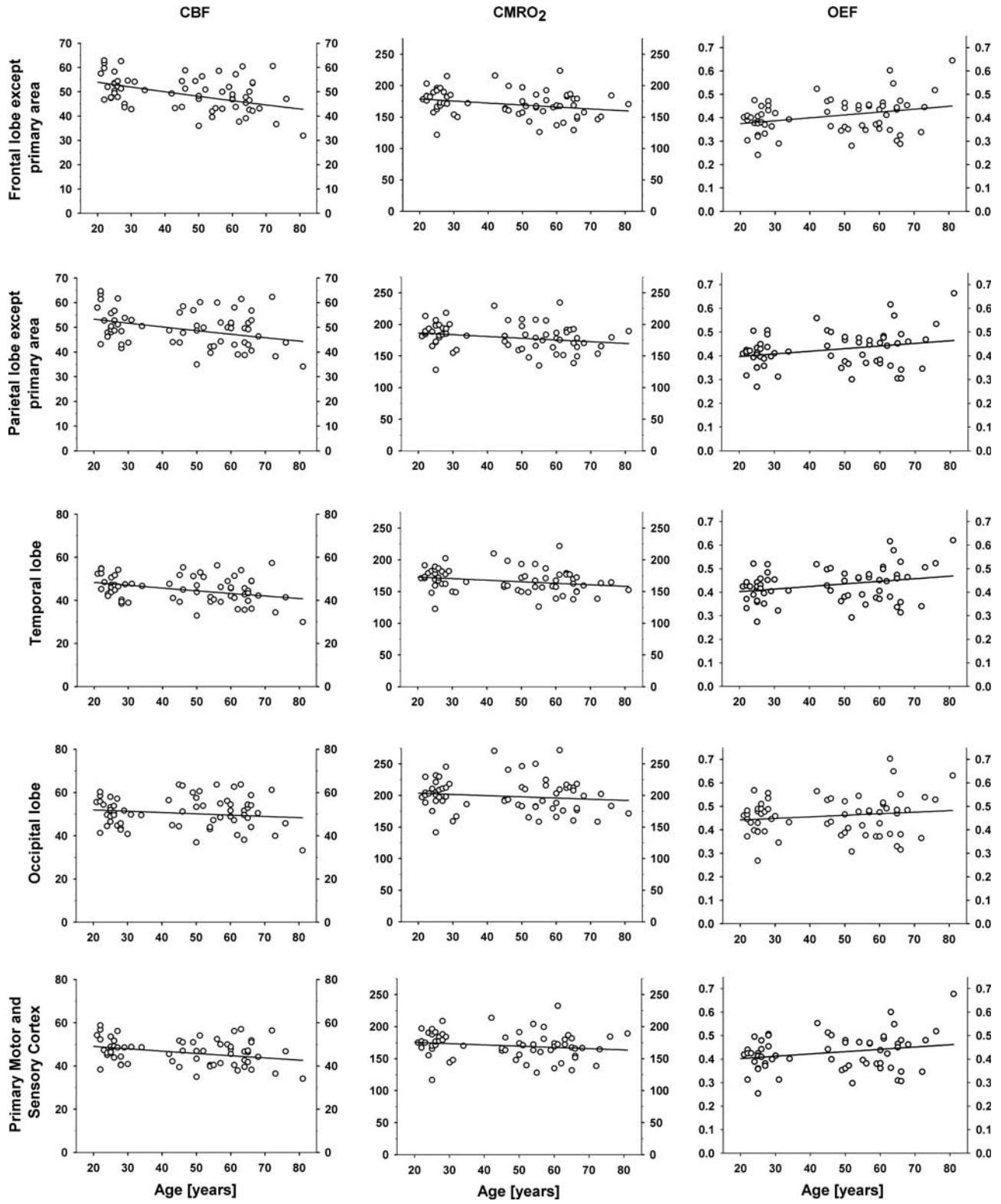

Figure 3 Scatter plots of cerebral blood flow (*CBF*), cerebral metabolic rate of oxygen consumption ($CMRO_2$), and oxygen extraction fraction (*OEF*) by volume-of-interest (VOI). Statistics for the regression lines are shown in Table 1. *CBF* (mL/100 g per minute), $CMRO_2$ (μmol/100 g per minute), *OEF* is a ratio.

2000, 2004; Gjedde *et al*, 2002). Thus, when brain energy metabolism declines, the steady-state estimates of *CBF* are expected to decline more than the steady-state estimates of $CMRO_2$ to be consistent with the nonlinear coupling relation expected of a homeostatic mechanism that maintains more or less

Table 2 *CBF*, $CMRO_2$, and *OEF* mean values in different age groups

	Young		*Middle age*		*Old*	
	Left	*Right*	*Left*	*Right*	*Left*	*Right*
CBF						
GM	49 (7.3)	51 (8.3)	48 (7.1)	49 (7.8)	46 (7.2)	47 (8.2)
F-M1	52 (6.2)	54 (7.0)	48 (5.7)	50 (6.4)	48 (5.2)	48 (6.3)
P-S1	52 (6.5)	53 (7.2)	50 (5.7)	50 (6.8)	49 (5.9)	49 (6.9)
T	47 (6.7)	48 (7.1)	46 (6.6)	47 (7.2)	43 (7.3)	44 (7.5)
O	50 (7.1)	53 (7.7)	53 (7.2)	55 (7.7)	51 (6.3)	53 (7.0)
M1S1	49 (6.4)	49 (7.5)	47 (5.9)	47 (6.7)	47 (5.1)	46 (6.6)
$CMRO_2$						
GM	176 (28)	178 (31)	174 (28)	175 (32)	168 (29)	169 (32)
F-M1	175 (22)	180 (23)	172 (21)	171 (22)	168 (20)	168 (21)
P-S1	185 (23)	186 (23)	181 (19)	185 (24)	177 (22)	180 (26)
T	169 (27)	173 (28)	167 (28)	168 (29)	159 (28)	164 (29)
O	196 (29)	209 (34)	202 (30)	212 (33)	197 (30)	207 (33)
M1S1	176 (21)	175 (26)	173 (20)	170 (22)	173 (23)	164 (23)
OEF						
GM	0.40 (0.05)	0.40 (0.05)	0.42 (0.04)	0.41 (0.05)	0.43 (0.05)	0.43 (0.05)
F-M1	0.38 (0.04)	0.37 (0.04)	0.41 (0.04)	0.40 (0.04)	0.42 (0.04)	0.41 (0.04)
P-S1	0.40 (0.04)	0.39 (0.04)	0.42 (0.04)	0.42 (0.04)	0.43 (0.04)	0.43 (0.04)
T	0.41 (0.05)	0.40 (0.05)	0.42 (0.05)	0.41 (0.04)	0.44 (0.05)	0.44 (0.05)
O	0.44 (0.05)	0.45 (0.05)	0.44 (0.04)	0.44 (0.04)	0.45 (0.05)	0.45 (0.06)
M1S1	0.40 (0.04)	0.40 (0.04)	0.42 (0.04)	0.42 (0.04)	0.43 (0.05)	0.42 (0.04)

CBF, cerebral blood flow; $CMRO_2$, cerebral metabolic rate of oxygen consumption; F-M1, frontal lobe without primary motor area; GM, cortical gray matter; M1S1, primary motor and somatosensory area; O, occipital lobe; *OEF*, oxygen extraction fraction; P-S1, parietal lobe without primary somatosensory area; T, temporal lobe.
Mean (s.d.) parametric values in different age groups; young 21 to 39, middle age 40 to 59, and old 60 to 81 years, shown for each hemisphere. *CBF* (mL/100 g per minute), $CMRO_2$ (μmol/100 g per minute), *OEF* is a ratio.

constant oxygen tensions in brain tissue and at the mitochondria. It is only when the values of *CBF* decline more than prescribed by the nonlinear coupling mechanism, or when the values of $CMRO_2$ decline less than prescribed, stay constant, or actually rise, that the extraction may rise to levels that are detrimental to adequate oxygen delivery. Lu *et al* (2011) reported declines of *CBF* estimates and increases of $CMRO_2$ estimates in normal healthy aging, which would be consistent with abnormal increases of *OEF* (from 0.34 to 0.40 in that study). However, the estimates of $CMRO_2$ may reflect the use of a constant literature value of arterial oxygen concentration of 8.337 mmol/L, which is not consistent with the possible changes of hemoglobin concentration with aging. In the present study, linear regression of hemoglobin concentration on age yielded a nonsignificant decline of hemoglobin concentration of 0.0079 mmol/L per year ($P = 0.149$).

Spatial Resolution

The methods as well as the spatial resolution of the tomograph used in the studies included in the present reanalysis were superior to those characteristic of previous reports. In earlier studies of changes of *CBF* and $CMRO_2$ during healthy aging, the authors generally had tomographs with resolutions in the 11 to 17 mm range (Itoh *et al*, 1990; Meltzer *et al*, 2000; Pantano *et al*, 1984), and they located regions of interest with diameters varying from 14 to 20 mm (Eustache *et al*, 1995; Leenders *et al*, 1990; Marchal *et al*, 1992; Yamaguchi *et al*, 1986). Because of some atrophy of the brains of aged subjects, the PVE arguably has a greater effect on the magnitude of parameter estimates from aged subjects than from younger subjects. The increased PVE of older subjects stems from sulcal widening. In young subjects with narrow sulci, PET resolution is less critical as a large sampling region would sample cortex on both sides of a sulcus. In aged subjects with advanced atrophy, however, a sampling region of the same size would on average cover more cerebrospinal fluid, thus leading to attenuation of the signal. Figure 5 shows representative examples of MR images from a young and an aged subject. Meltzer *et al* (2000) found that the significant decline of *CBF* with aging disappeared when they corrected the data for the PVE. However, in this study, the in-plane FWHM was no less than 10.3 mm. To minimize loss of resolution in the present study, we analyzed the data with a FWHM of 6 mm in both the VOI and age group analyses, which is a resolution that is closer to the average thickness of the cerebral cortex of 2.5 to 3 mm (Pakkenberg and Gundersen, 1997; Rabinowicz

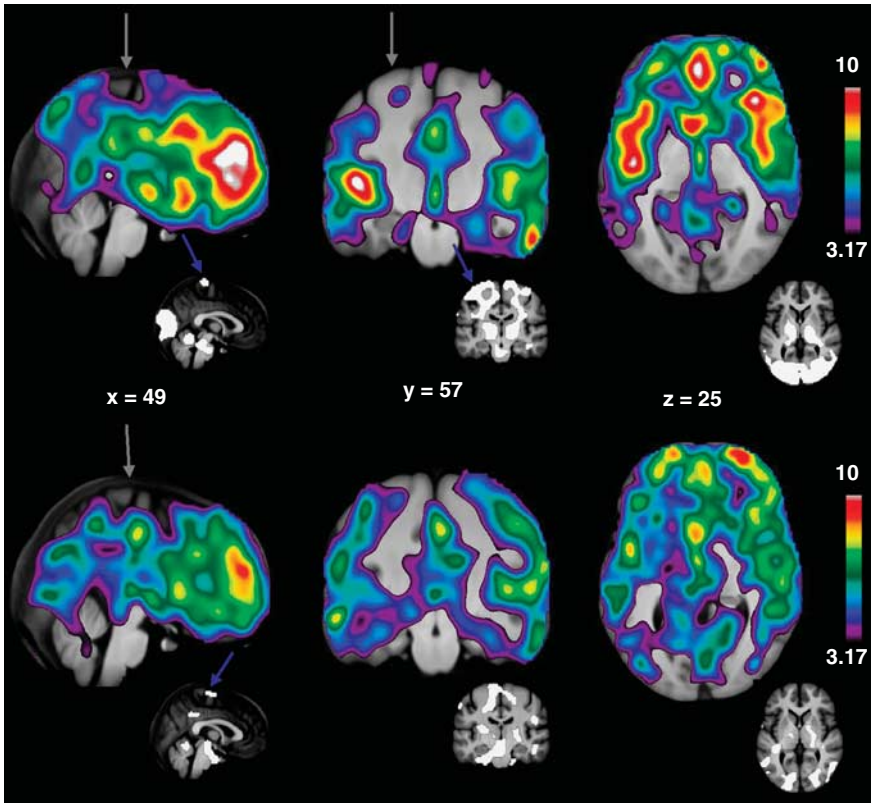

Figure 4 *T*-maps of cerebral blood flow (*CBF*) (top) and cerebral metabolic rate of oxygen consumption ($CMRO_2$) (bottom) relative decreases as a function of age. *T*-values are shown on the right, threshold $P = 0.05$, corrected. The most significant decreases in both *CBF* and $CMRO_2$ are seen in the superior frontal gyrus. Small insets display masks used in ratio normalization, these masks represent areas that are preserved during aging. Gray arrows indicate medial superior part of the central sulcus, which is surrounded by primary motor and somatosensory areas and is preserved during aging (blue arrows).

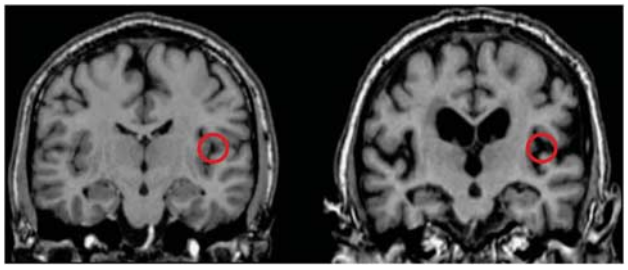

Figure 5 Illustration of sulcal widening in old age. Magnetic resonance (MR) images of two men are shown, on the left is a 26 year old and on the right an 81 year old. If large, fixed-sized volumes-of-interest (VOIs) or regions of interest (ROIs) (14 to 20 mm in earlier studies) are used to sample values from the corresponding positron emission tomography (PET) images, a larger proportion of the sampling area would include sulcal cerebrospinal fluid (CSF) in older subjects.

et al, 2002). Part of the decline of the *CBF* and $CMRO_2$ values observed with the present reanalysis still could be attributable to PVE, but the observation that *CBF* values declined while $CMRO_2$ values remained unchanged in a region such as M1S1, and that the *OEF* changed with age in some regions only, implies that not all declines of the signal was due to atrophy.

Individual Gray Matter Masks

Masks defined on an atlas brain depend for their accuracy on the quality of coregistration of the atlas brain and on the individual PET images. A potential bias of this method is age-associated atrophy as old brains are smaller than young brains (Pakkenberg and Gundersen, 1997). This fact could influence the adequacy of the fit between atlas and individual brain images. A common approach in early PET studies of aging was the outlining of VOIs directly on the PET images. This method introduces a bias when the investigator samples areas with a strong or a weak signal, depending on the aim of the study. To avoid these pitfalls in this reanalysis, we chose as a third option an automated algorithm for extraction of VOIs that ensured uniform sampling with individualized masks (exemplified in Figure 1), based on magnetic resonance imaging-derived anatomical knowledge of individual subjects' brains.

Volume-of-Interest Analysis

The magnitude of the reduction of *CBF* estimates in frontal and parietal cortices without the primary

motor and somatosensory areas, and the temporal cortex, is largely consistent with the results of earlier studies (Leenders *et al*, 1990; Lenzi *et al*, 1981; Marchal *et al*, 1992; Martin *et al*, 1991; Pantano *et al*, 1984). Leenders *et al* (1990) found decreases only in frontal cortex and insula and unchanged *CBF* in temporal and parietal cortices, possibly due to low resolution. In agreement with all previous studies, occipital cortex had unchanged *CBF* also in the present reanalysis. Primary motor and somatosensory areas displayed some decrease with age, although the slope was less steep than in associative cortices.

We found that $CMRO_2$ estimates decline in primary motor cortex (F-M1) and tend to decline in primary sensory (P-S1) and temporal cortices, while occipital and primary motor (M1S1) cortices remain unchanged during aging. This finding generally is consistent with recent as well as earlier findings (Ibaraki *et al*, 2010; Leenders *et al*, 1990; Marchal *et al*, 1992).

The significant increases of *OEF* found in the F-M1 and P-S1 cortices and in temporal cortex is the most important difference from the results of earlier studies. In three studies, the authors reported no effect of aging on *OEF* (Ibaraki *et al*, 2010; Marchal *et al*, 1992; Pantano *et al*, 1984), while in one study, the authors reported increases in frontal cortex and insula (Leenders *et al*, 1990). We argue that the large study population and age span, and sampling of parametric data with MR-derived individual masks give credibility to the present results. Detecting a change of *OEF* is made difficult by the presence of biological noise in both the $CMRO_2$ and *CBF* estimates and the risk of compounding the noise in the calculation of *OEF*. Small study populations, narrow age ranges, and attenuation of the PET signal by PVE all lower the power of the regression analysis and could have impaired the detection of age-related changes in earlier studies.

Voxel-Based Analysis

In the present reanalysis, we found an apparent coincidence between areas with unchanged *CBF* and $CMRO_2$ during healthy aging and areas that are heavily myelinated and highly functionally specialized as well as known to be least affected in neurodegenerative diseases such as Alzheimer's and Parkinson's diseases (Braak *et al*, 2006). In contrast, we found estimates of diminished *CBF* and increased *OEF* in associative areas, reported by Braak *et al* (2006), to be the parts of the brain most vulnerable to unhealthy aging. We interpret this result as an indication that lowering of *CBF* values with concomitant increases of *OEF* can be one attributing factor, among others, to unhealthy aging of the brain, perhaps related to changes of neurovascular coupling. In the case of Alzheimer's disease, these changes can be related to amyloid deposits (Smith and Greenberg, 2009).

At the threshold of 60% extraction, oxygen delivery to the tissue becomes compromised with resulting impairment of oxidative phosphorylation and adequate ATP regeneration. We found that values of $CMRO_2$ also tend to be decreased in associative regions, but to less extent than was the values of *CBF* (hence the increased *OEF* revealed by the VOI analysis). The increased *OEF* potentially leaves the neurons susceptible to inadequate energy homeostasis, as argued by Nicholls (2008). Neurons in associative areas of the brain have less myelin than neurons in primary areas and consequently require higher rates of energy turnover for signaling (Hildebrand *et al*, 1993). This increased energy requirement, superimposed on reduced capacity for ATP production, may leave the cells susceptible to apoptosis.

Limitations

In the voxel-based analyses, smoothing of data to 12 mm FWHM was necessary to minimize noise. The lower resolution can explain the decreased values of *CBF* and $CMRO_2$ in central areas close to ventricles and the longitudinal fissure due to the PVE, without affecting the lateral aspects of the hemispheres. Meltzer *et al* (2000) found that PVE correction eliminated the different values of *CBF* in the groups of young and old subjects. The present data were not corrected for PVE, but the resolution (FWHM 6 mm) of the parametric images nevertheless exceeded that of previous studies. However, the residual PVE could influence the results and account for part of the observed decline of estimated values. The main finding in this study is that *OEF* shows increases in associative cortices. Theoretically, $CMRO_2$ could be unchanged (or even increased) during aging, while *CBF* could be diminished to a lesser degree by aging than observed in the data, but still this would not change the relationship between the two variables, that is, *OEF*. The *CBF* and $CMRO_2$ measurements were performed on the same subjects, with the same methodology, with measurements made only a few minutes apart, so we have no reason to suspect that PVE would affect one of the variables more than the other. The different rates of decline of *CBF* and $CMRO_2$ (reflected in the increased *OEF*), thus, argue that although some of the observed decline could be due to PVE, at least some of the decrease in *CBF* must be due to a real decline in blood flow.

As subjects were not screened for vascular encephalopathy, it is possible that some of the older subjects had undetected cerebrovascular changes that may contribute to some decline of *CBF*.

The crosssectional design makes it impossible to distinguish between effects of aging *per se* and the effects of being born at different times (Miller and Corsellis, 1977). We observed large variability of both *CBF* (COV (coefficient of variation) 0.15) and $CMRO_2$ (COV 0.12), comparable to the variation observed in

other studies (Ibaraki *et al*, 2010; Leenders *et al*, 1990; Meltzer *et al*, 2000). This variation makes it difficult to ascertain whether the aging effect is due to some individuals having large changes with age and others having unchanged values, or whether the changes apply to everyone to some degree. Also, it is not possible at this time to determine whether the great variability reflects variable mitochondrial efficiency (uncoupling) in different individuals, or whether the degree of uncoupling is similar in all individuals. The average degree of uncoupling in the human brain appears to be close to 75% but is not related to values of body mass index, as it is in the body as a whole (Gjedde *et al*, 2011).

Conclusions

We found estimates of *CBF* and to less extent estimates of $CMRO_2$ to decrease with age in extended regions of the brain, with relative sparing of primary sensory-motor and occipital cortices. This result of the reanalysis is consistent with evidence from previous studies, although we found more widespread declines of the estimates of both *CBF* and $CMRO_2$. The widespread increases of *OEF* in F-M1, P-S1, and temporal cortices are novel findings. The large study population and the automated, individualized VOI sampling contribute to the significance of this result. The spatially distributed declines of values of *CBF* and $CMRO_2$ revealed by the voxel-based analysis and the consequent spatial distribution of increased values of *OEF* coincide with areas known to be vulnerable in AD and PD.

Although functional magnetic resonance imaging and other modalities for brain imaging have been used increasingly over the past decade, PET remains the gold standard of regionally measured absolute blood flow and metabolism measurements. To distinguish further between the effects of aging and being born at different times, and to evaluate interindividual variability, future studies would focus on estimates of actual ATP turnover and a prospective longitudinal design of the studies.

Disclosure/conflict of interest

The authors declare no conflict of interest.

References

Ashkanian M, Gjedde A, Mouridsen K, Vafaee M, Hansen KV, Ostergaard L, Andersen G (2009) Carbogen inhalation increases oxygen transport to hypoperfused brain tissue in patients with occlusive carotid artery disease: increased oxygen transport to hypoperfused brain. *Brain Res* 1304:90–5

Blomqvist G (1984) On the construction of functional maps in positron emission tomography. *J Cereb Blood Flow Metab* 4:629–32

Borghammer P, Aanerud J, Gjedde A (2009*a*) Data-driven intensity normalization of PET group comparison studies is superior to global mean normalization. *Neuroimage* 46:981–8

Borghammer P, Cumming P, Aanerud J, Gjedde A (2009*b*) Artefactual subcortical hyperperfusion in PET studies normalized to global mean: lessons from Parkinson's disease. *Neuroimage* 45:249–57

Borghammer P, Jonsdottir KY, Cumming P, Ostergaard K, Vang K, Ashkanian M, Vafaee M, Iversen P, Gjedde A (2008) Normalization in PET group comparison studies–the importance of a valid reference region. *Neuroimage* 40:529–40

Braak H, Rub U, Schultz C, Del Tredici K (2006) Vulnerability of cortical neurons to Alzheimer's and Parkinson's diseases. *J Alzheimers Dis* 9:35–44

Burns A, Tyrrell P (1992) Association of age with regional cerebral oxygen utilization: a positron emission tomography study. *Age Ageing* 21:316–20

Buxton RB, Frank LR (1997) A model for the coupling between cerebral blood flow and oxygen metabolism during neural stimulation. *J Cereb Blood Flow Metab* 17:64–72

Collins DL, Evans AC (1997) Animal: validation and applications of nonlinear registration-based segmentation. *Int J Pattern Recognit Artif Intell* 11:1271–94

Collins DL, Holmes CJ, Peters TM, Evans AC (1995) Automatic 3D model-based neuroanatomical segmentation. *Human Brain Mapp* 3:190–208

Eustache F, Rioux P, Desgranges B, Marchal G, Petit-Taboue MC, Dary M, Lechevalier B, Baron JC (1995) Healthy aging, memory subsystems and regional cerebral oxygen consumption. *Neuropsychologia* 33:867–87

Gjedde A (1997) The relation between brain function and cerebral blood flow and metabolism. In: *Cerebrovascular Disease*, (HH B, ed) Lippincott-Raven: Philadelphia, 23–40

Gjedde A, Aanerud J, Peterson E, Ashkanian M, Iversen P, Vafaee M, Moller A, Borghammer P (2011) Variable ATP yields and uncoupling of oxygen consumption in human brain. *Adv Exp Med Biol* 701:243–8

Gjedde A, Johannsen P, Cold GE, Ostergaard L (2005) Cerebral metabolic response to low blood flow: possible role of cytochrome oxidase inhibition. *J Cereb Blood Flow Metab* 25:1183–96

Gjedde A, Keiding S, Vilstrup H, Iversen P (2010) No oxygen delivery limitation in hepatic encephalopathy. *Metab Brain Dis* 25:57–63

Gjedde A, Marrett S, Vafaee M (2002) Oxidative and nonoxidative metabolism of excited neurons and astrocytes. *J Cereb Blood Flow Metab* 22:1–14

Hildebrand C, Remahl S, Persson H, Bjartmar C (1993) Myelinated nerve-fibers in the CNS. *Progress Neurobiol* 40:319–84

Ibaraki M, Shinohara Y, Nakamura K, Miura S, Kinoshita F, Kinoshita T (2010) Interindividual variations of cerebral blood flow, oxygen delivery, and metabolism in relation to hemoglobin concentration measured by positron emission tomography in humans. *J Cereb Blood Flow Metab* 30:1296–305

Ito H, Yokoyama I, Iida H, Kinoshita T, Hatazawa J, Shimosegawa E, Okudera T, Kanno I (2000) Regional differences in cerebral vascular response to PaCO2 changes in humans measured by positron emission tomography. *J Cereb Blood Flow Metab* 20:1264–70

Itoh M, Hatazawa J, Miyazawa H, Matsui H, Meguro K, Yanai K, Kubota K, Watanuki S, Ido T, Matsuzawa T

(1990) Stability of cerebral blood flow and oxygen metabolism during normal aging. *Gerontology* 36:43–8

Iversen P, Sorensen M, Bak LK, Waagepetersen HS, Vafaee MS, Borghammer P, Mouridsen K, Jensen SB, Vilstrup H, Schousboe A, Ott P, Gjedde A, Keiding S (2009) Low cerebral oxygen consumption and blood flow in patients with cirrhosis and an acute episode of hepatic encephalopathy. *Gastroenterology* 136: 863–71

Kety SS (1956) Human cerebral blood flow and oxygen consumption as related to aging. *J Chronic Dis* 3:478–86

Kety SS, Schmidt CF (1945) The determination of cerebral blood flow in man by the use of nitrous oxide in low concentrations. *Am J Physiol* 143:53–66

Kety SS, Schmidt CF (1948) The nitrous oxide method for the quantitative determination of cerebral blood flow in man—theory, procedure and normal values. *J Clin Invest* 27:476–83

Lawson G, Hanson RJ (1974) *Solving Least Squares Problems*. Prentice Hall Inc.: New Jersey

Leenders KL, Perani D, Lammertsma AA, Heather JD, Buckingham P, Healy MJ, Gibbs JM, Wise RJ, Hatazawa J, Herold S, Beaney RP, Brooks DJ, Spinks T, Rhodes C, Frackowiak RSJ, Jones T (1990) Cerebral blood flow, blood volume and oxygen utilization. Normal values and effect of age. *Brain* 113(Part 1):27–47

Lenzi GL, Frackowiak RS, Jones T, Heather JD, Lammertsma AA, Rhodes CG, Pozzilli C (1981) CMRO2 and CBF by the oxygen-15 inhalation technique Results in normal volunteers and cerebrovascular patients. *Eur Neurol* 20:285–90

Lu H, Xu F, Rodrigue KM, Kennedy KM, Cheng Y, Flicker B, Hebrank AC, Uh J, Park DC (2011) Alterations in cerebral metabolic rate and blood supply across the adult lifespan. *Cereb Cortex* 21:1426–34

Marchal G, Rioux P, Petit-Taboue MC, Sette G, Travere JM, Le Poec C, Courtheoux P, Derlon JM, Baron JC (1992) Regional cerebral oxygen consumption, blood flow, and blood volume in healthy human aging. *Arch Neurol* 49:1013–20

Martin AJ, Friston KJ, Colebatch JG, Frackowiak RS (1991) Decreases in regional cerebral blood flow with normal aging. *J Cereb Blood Flow Metab* 11:684–9

Meltzer CC, Cantwell MN, Greer PJ, Ben-Eliezer D, Smith G, Frank G, Kaye WH, Houck PR, Price JC (2000) Does cerebral blood flow decline in healthy aging? A PET study with partial-volume correction. *J Nucl Med* 41:1842–8

Miller AK, Corsellis JA (1977) Evidence for a secular increase in human brain weight during the past century. *Ann Hum Biol* 4:253–7

Mintun MA, Raichle ME, Martin WR, Herscovitch P (1984) Brain oxygen utilization measured with O-15 radiotracers and positron emission tomography. *J Nucl Med* 25:177–87

Møller A, Roepstorff A, Cumming P, Pedersen GF, Bailey C, Gjedde A (2006) *Cerebrometabolic Effects of Non-Ionizing Radiation from Cell Phones*. International Conference On Brain Energy Metabolism, poster session: Lausanne

Nemoto EM, Yonas H, Chang Y (2003) Stages and thresholds of hemodynamic failure. *Stroke* 34:2–3

Nicholls DG (2008) Oxidative stress and energy crises in neuronal dysfunction. *Mitochondria and Oxidative Stress in Neurodegenerative Disorders* 1147:53–60

Ohta S, Meyer E, Fujita H, Reutens DC, Evans A, Gjedde A (1996) Cerebral [15O]water clearance in humans determined by PET: I. Theory and normal values. *J Cereb Blood Flow Metab* 16:765–80

Ohta S, Meyer E, Thompson CJ, Gjedde A (1992) Oxygen consumption of the living human brain measured after a single inhalation of positron emitting oxygen. *J Cereb Blood Flow Metab* 12:179–92

Pakkenberg B, Gundersen HJ (1997) Neocortical neuron number in humans: effect of sex and age. *J Comp Neurol* 384:312–20

Pantano P, Baron JC, Lebrun-Grandie P, Duquesnoy N, Bousser MG, Comar D (1984) Regional cerebral blood flow and oxygen consumption in human aging. *Stroke* 15:635–41

Rabinowicz T, Petetot JM, Gartside PS, Sheyn D, Sheyn T, de CM (2002) Structure of the cerebral cortex in men and women. *J Neuropathol Exp Neurol* 61:46–57

Raichle ME, Martin WR, Herscovitch P, Mintun MA, Markham J (1983) Brain blood flow measured with intravenous H2(15)O. II. Implementation and validation. *J Nucl Med* 24:790–8

Smith EE, Greenberg SM (2009) Beta-amyloid, blood vessels, and brain function. *Stroke* 40:2601–6

Suwa K (1992*a*) Analysis of oxygen transport to the brain when two or more parameters are affected simultaneously. *J Anesth* 6:297–304

Suwa K (1992*b*) Analysis of oxygen transport and oxygen utilization combined. *J Anesth* 6:51–6

Takada H, Nagata K, Hirata Y, Satoh Y, Watahiki Y, Sugawara J, Yokoyama E, Kondoh Y, Shishido F, Inugami A, Fujita H, Ogawa T, Murakami M, Lida H, Kanno I (1992) Age-related decline of cerebral oxygen metabolism in normal population detected with positron emission tomography. *Neurol Res* 14:128–31

Vafaee MS, Gjedde A (2000) Model of blood-brain transfer of oxygen explains nonlinear flow-metabolism coupling during stimulation of visual cortex. *J Cereb Blood Flow Metab* 20:747–54

Vafaee MS, Gjedde A (2004) Spatially dissociated flow-metabolism coupling in brain activation. *Neuroimage* 21:507–15

Worsley KJ, Liao CH, Aston J, Petre V, Duncan GH, Morales F, Evans AC (2002) A general statistical analysis for fMRI data. *Neuroimage* 15:1–15

Worsley KJ, Marrett S, Neelin P, Vandal AC, Friston KJ, Evans AC (1996) A unified statistical approach for determining significant signals in images of cerebral activation. *Hum Brain Mapp* 4:58–73

Yakushev I, Hammers A, Fellgiebel A, Schmidtmann I, Scheurich A, Buchholz HG, Peters J, Bartenstein P, Lieb K, Schreckenberger M (2009) SPM-based count normalization provides excellent discrimination of mild Alzheimer's disease and amnestic mild cognitive impairment from healthy aging. *Neuroimage* 44:43–50

Yamaguchi T, Kanno I, Uemura K, Shishido F, Inugami A, Ogawa T, Murakami M, Suzuki K (1986) Reduction in regional cerebral metabolic rate of oxygen during human aging. *Stroke* 17:1220–8